

PAPER • OPEN ACCESS

Additively manufactured Ti-6-4 ELI customized subperiosteal dental exo-implant

To cite this article: G Z Mukanov *et al* 2021 *IOP Conf. Ser.: Mater. Sci. Eng.* **1029** 012100

View the [article online](#) for updates and enhancements.



The Electrochemical Society
Advancing solid state & electrochemical science & technology
2021 Virtual Education

Fundamentals of Electrochemistry:
Basic Theory and Kinetic Methods
Instructed by: **Dr. James Noël**
Sun, Sept 19 & Mon, Sept 20 at 12h–15h ET

Register early and save!



Additively manufactured Ti-6-4 ELI customized subperiosteal dental exo-implant

G Z Mukanov^{1,*}, S I Stepanov¹ and Yu N Loginov^{1,2}

¹Ural Federal University named after the first President of Russia B.N. Yeltsin, Ekaterinburg, Russia

²Institute of Metal Physics of Ural Branch of Russian Academy of Sciences, Ekaterinburg, Russia

*corresponding author: usuals@bk.ru

Abstract. The role of digital technologies in the manufacture of metal products with complex geometry used in medicine is discussed. A sequence of actions is proposed to obtain a dental implant from biocompatible titanium alloy powder using the additive manufacturing based on features of human jaw anatomy. The boundary conditions for the problem are stated based on the literature data for jaw loading. The strength calculations by finite element method enabled the topological optimization of the implant. The production features of subperiosteal dental exo-implant using electron beam (EBM) melting are presented. Microstructure implant produced from Ti-6-4 ELI powder by EBM was examined.

1. Introduction

Digital technologies determine the direction of development of modern industry. Such production methods as additive manufacturing (AM) are constantly being improved. These technologies make it possible to create complex structures based on a given three-dimensional model obtained by solid modeling or reverse prototyping using selective melting of the powders, e.g. powder bed fusion (PBF). Selective laser melting (SLM) and electron-beam melting (EBM) are among such methods, which have found its place in the creation of high-precision custom-made implants used in traumatology and orthopedics [1-3]. A significant number of implants are made of titanium or alloys based on it [4, 5]. Many nuances should be taken into account for patient specific implants starting from the anatomical features of the body and ending with the tailoring the mechanical properties such as strength and elastic modulus of the implant.

There is a possibility to comprehensively estimate the strength characteristics of the final product using special software based on the finite element method (FEM), due to the fact that refined 3D models can be created in course of the additive manufacturing process [6, 7]. The difference in thickness of implant structural elements due to the heterogeneous distribution of the external load is taken into account in FEM simulation. This enables to make topological optimization based on the obtained stress-strain state. The purpose of the study is to produce custom-made subperiosteal dental exo-implant and to estimate its stress state under conditions of chewing loads.

2. Material and Methods

The first step to personalize a bone implant and to match the bone surface profile of a specific patient is to obtain computed tomography (CT) data from the patient. Based on two-dimensional CT images



Content from this work may be used under the terms of the [Creative Commons Attribution 3.0 licence](https://creativecommons.org/licenses/by/3.0/). Any further distribution of this work must maintain attribution to the author(s) and the title of the work, journal citation and DOI.

obtained, a virtual 3D model is generated that exactly corresponds to the anatomical features of a particular bone fragment. In order to mount the implant to the bone, the holes for the screws are determined by the features of the anatomical structure of the maxillofacial system. The upper jaw differs from the lower by the presence of air cavities called the maxillary sinuses. The volume and shape of the maxillary sinuses are individual. If they are small with thick walls, a general surgery of screw dental implants is not needed. However, the large thin-walled cavities make traditional methods of dental implantology impossible. Otherwise an artificial tooth can get into the air cavity when chewing.

A CT segmentation process includes the 2D images processing, creating a 3D model by combining the images in three dimensions (axial, sagittal, frontal) and selecting an interval on the density scale for a particular bone. The design of 3D masks based on the segmentation was carried out in the freely available InVesalius software, which allows processing each tomographic layer with an accuracy of 0.025 mm (Fig. 1, stage 1). The maxillary point mask must be transformed into STL format (an abbreviation of "stereolithography"), which represents a combination of triangular elements of the facet body of the mask (Fig. 1, stage 2). The stereolithographic model of the jaw serves as a basis for creating an adjacent surface topology of the patient specific implant. An experienced dental surgeon, who will finally perform a surgery using this implant, is implied to take part in the design of customized implant. Based on his recommendations, a back bracket was designed as a part of the implant, which helps to limit the displacement of the implant along the bone surface. Thus, a solid-state CAD model of a patient-specific subperiosteal dental exo-implant was created (Fig. 1, stage 3). According to the previous studies [7, 8], the following boundary conditions were taken and strength calculations were carried out using the finite element method (FEM), based on which the final implant design was adjusted (Fig. 1, stage 4). The diameter of the base of the abutment of 6 mm was set in order to provide the necessary area at the contact with base plate and to prevent a localization of equivalent stresses [7].

At the next step, the STL assembly model of the upper jaw and implant is translated into the format of the corresponding 3D printer and configure the synthesis of the final the product. In this case, the EBM machine was employed (Fig. 1, stage 5).

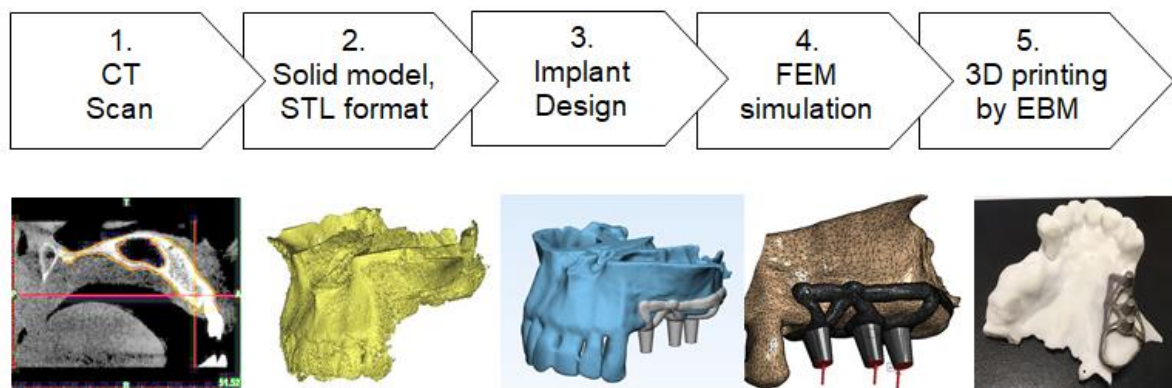


Figure 1. Additive manufacturing route of subperiosteal dental exo-implant

A tetragonal mesh was generated with the number of elements 90,000 to describe a complex mathematical model of the implant for FEM simulation. A verification for the absence of mesh intersections was made with the Element quality parameter.

The boundary conditions were determined based on the maximum load of the masticatory muscles of a human [8]. A distributed pressure of 38 MPa was applied to each abutment site. As indicated in [7], the angle between the load vector and the abutment surface of 20° was set (Fig. 2). Thus, the load was distributed over 3 components, along X: $P = 15$ MPa, along Y: $P = 0$, along Z: $P = 36$ MPa. A «body-ground» contact was chosen between the internal contact surface of the implant and the surface of the jaw to simulate the connection of the implant with the bone. The rigidity of the simulated surface of the lower

jaw of 13700 N/mm^2 was taken, which corresponded to the rigidity of the surface of the upper jaw bone (13.7 GPa). The screws were defined as non-deformable beam elements with a radius of $500 \text{ }\mu\text{m}$.

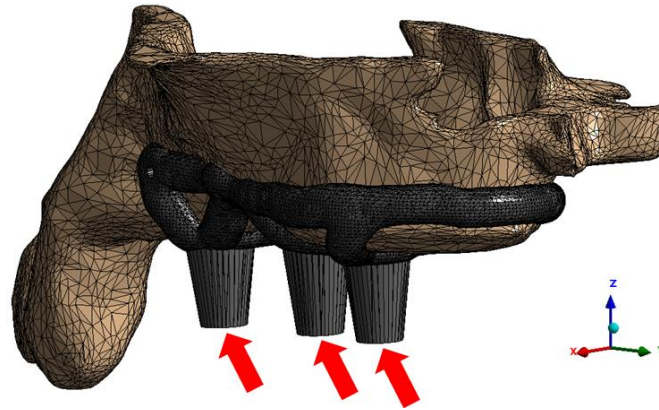


Figure 2. Direction of external load indicated with red arrows applied to the implant mounted on the fragment of the jaw with the specified coordinate system

3. Results and Discussion

According to the results of the FEM simulation, the stress-strain diagram of the dental implant was obtained. The equivalent von Mises stresses have a very homogeneous distribution over the entire body of the implant without evident localizations as can be seen from Fig. 3.

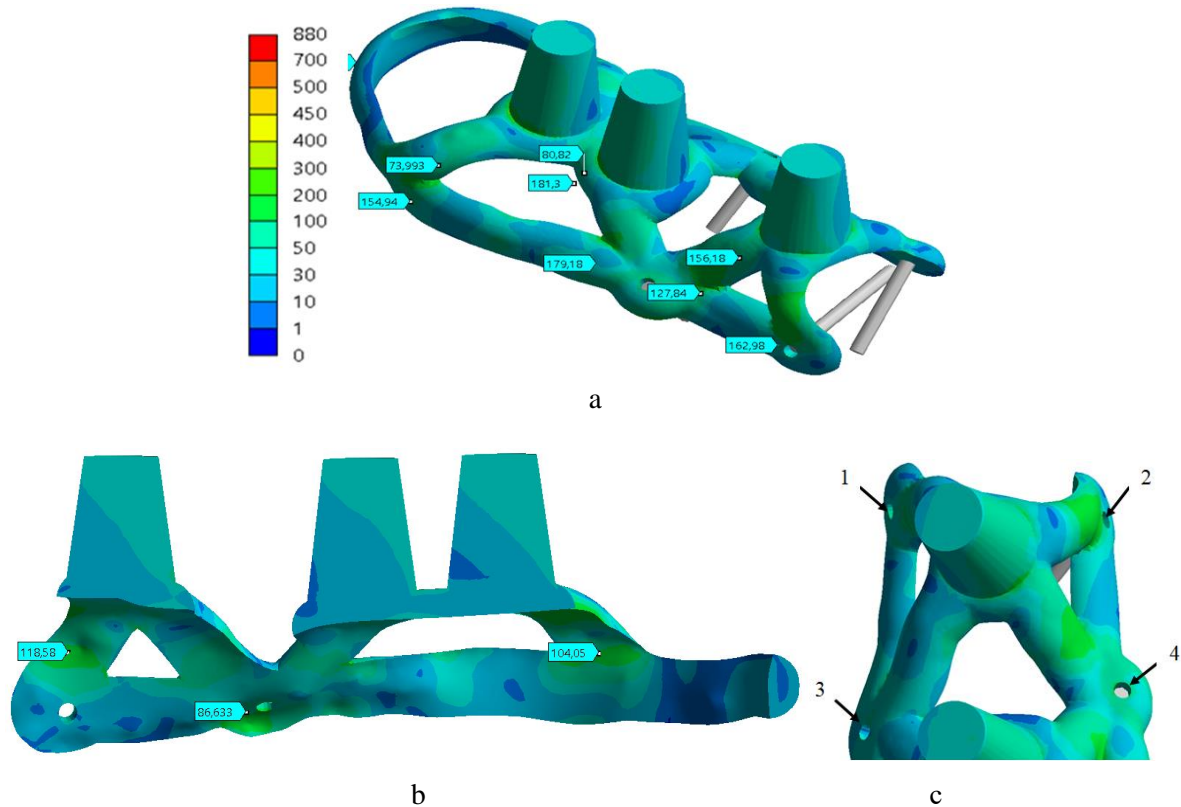


Figure 3. Mises equivalent stress field distribution in 3D projection (a), longitudinal cross-section (b) and location of screw joints in the implant (c)

The yield strength of the Ti-6-4 ELI of 880 MPa is taken as the strength criteria. The maximum local stresses arise in the elements aligned with the external load vectors and amount 168 MPa, as well as in the regions, where the dental abutments are fixed (181 MPa). The safety factor in these regions is approximately 5, which indicates the reliability of this design in dangerous section. Equivalent stresses in the field of mounting holes take low value, which prove that the holes are positioned correctly.

The back bracket described above fixed the implant in the Y direction in the chosen coordinate system (Fig. 3). This is based on the analysis of the stress-strain state in a longitudinal sectional view (Fig. 3 b), for which the stress fields take higher values from the side where the longitudinal degree of freedom of the implant is limited.

In order to gain a more complete understanding of the displacement of the implant relative to the jaw, the loads experienced by the screws in the threaded connection with the bone were evaluated. Due to the multidisciplinary capabilities of the Ansys Workbench, a user output of the results was specified in the postprocessing calculation module. Thus, the screw number 1 experiences an axial load of 12 N (Fig. 3 c); number 2 - 8 N; number 3 - 6 N; number 4 - 21 N. None of these loads exceeded the test load for a given threaded connection. Therefore, the implant is rigidly fixed to the surface of the jaw.

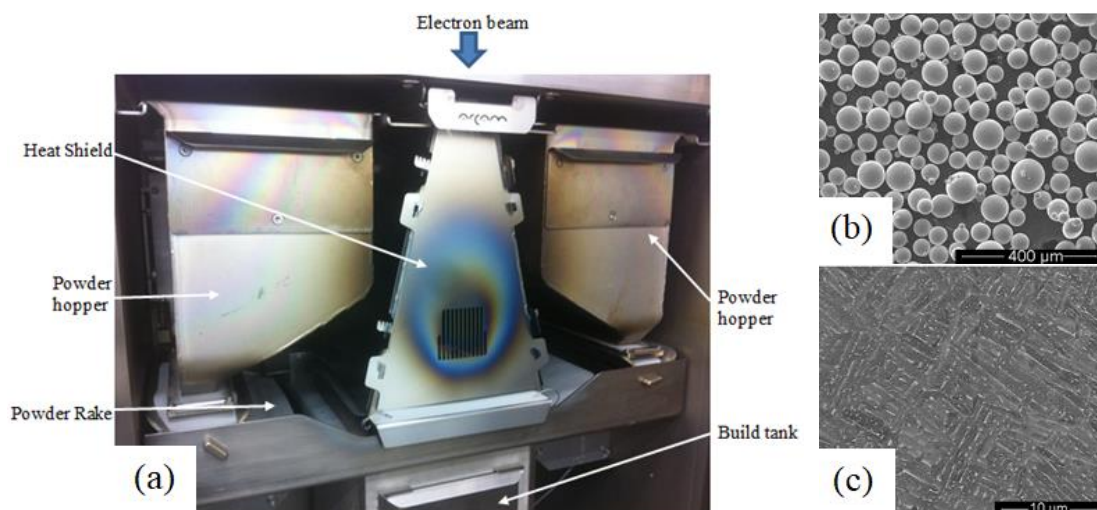


Figure 4. Schematic drawing of an Arcam A2X electron beam melting system (a), powder image (b) and as-built Ti-6-4 ELI structure (c)

According to the results of the static loading simulation, the model of subperiosteal dental exo-implant obtained by the above algorithm was sent to a 3D printing machine (Fig. 4 a). An Arcam A2X EBM machine under vacuum of 10^{-4} mbar or greater was employed to carry out the electron beam melting providing an ideal contamination-free environment for manufacturing of reactive materials, such as titanium alloys, that have a high affinity to interstitials. Ti-6Al-4V ELI powder with a particle size in the range of 45–120 μm , was utilized as a printing material for the research (Fig. 4 b). According to [9], the usage of smaller fraction of powders can result in instability of the process, whereas the coarser ones is limited by the layer thickness. The fine particles and small satellites can reduce the flowability, density and electric conductivity of the processed material.

EBM provides a faster build rate than DED and SLM due to its superior energy input and fast scan speed [10]. The main shortcoming is its inferior surface quality. The high build temperature of 600–750 $^{\circ}\text{C}$ resulted in a stable structure characterized by lamellar hcp α -phase (dark regions) with interlayers of bcc β -phase (bright plates) shown in Fig. 4 c. Therefore, the structure stabilizing and stress relief heat treatments were not required. A 3D printed jaw prototype made of plastic powder was used for verification analysis of the landing of a subperiosteal dental exo-implant (Fig. 5). The implant was fixed on a plastic jaw without backlashes and displacements.

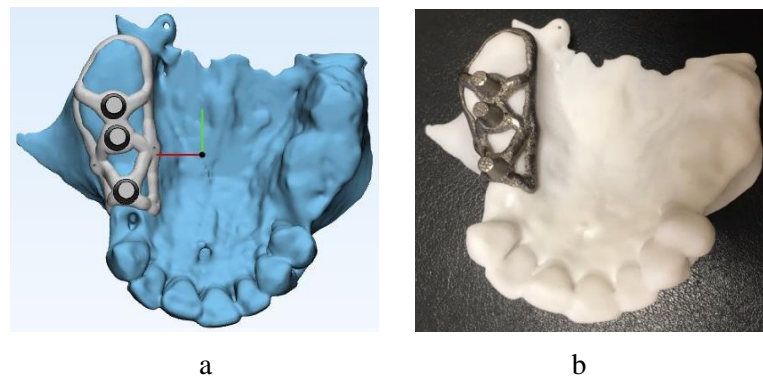


Figure 5. Subperiosteal dental exo-implant: (a) designed 3D model, (b) finished AM product mounted on a plastic bone prototype

Therefore, the simulation results presented in this study and the applicable foundations of the design of biomechanical systems can be used for further development in the field of AM of dental patient specific implants.

4. Conclusion

The algorithm of the design and manufacture of custom-made subperiosteal dental exo-implant was proposed based on digital technologies including finite element simulation and electron beam melting. Sufficient assurance coefficient was verified for the dental implant of a complex geometry by the calculations of the stress-strain state using the finite element method of the implant. The precise dimensions and stable ($\alpha+\beta$)-microstructure of the implant were provided by EBM.

The study was supported by the Grant of the Russian Science Foundation № 18-13-00220

References

- [1] Ilea A et al. 2019 *An in vitro Study on the Biocompatibility of Titanium Implants Made by Selective Laser Melting*, Biotechnology and Bioprocess Engineering, 24, pp 782-792
- [2] Xu J Y et al. 2016 *Improved bioactivity of selective laser melting titanium: Surface modification with micro-/nano-textured hierarchical topography and bone regeneration performance evaluation*, Materials Sci. and Eng., 68, pp 229-240
- [3] Popov V V, Muller-Kamskii G, Kovalevsky A 2018 *Design and 3D-printing of titanium bone implants: brief review of approach and clinical cases*, Biomed. Eng. Lett., 8, pp 337–344
- [4] Loginov Y N et al. 2018 *SLM parameters on the structure and properties of CP-Ti*, AIP Conference Proceedings, 2053 040052.
- [5] Mommaerts M Y 2017 *Additively manufactured sub-periosteal jaw implants*, International J. of Oral and Maxill of acial Surgery, 7, pp 938-940
- [6] Somasundaram P et al. 2020 *Biomechanics of all oplastic mandible reconstruction using biomaterials: The effect of implant design on stress concentration influences choice of material*, J. of the Mechanical Behavior of Biomedical Materials, 103, 103548
- [7] Golodnov A I Loginov Y N Stepanov S.I. 2018 *Numeric loading simulation of titanium implant manufactured using 3d printing*, Solid State Phenomena, 284, pp 380-385
- [8] Takaki P Vieira M Bommarito S 2014 *Maximum Bite Force Analysis in Different Age Groups*, Int Arch Otorhinolaryngol, 18, pp 272–276
- [9] Popov V V et al. 2018 *The effect of powder recycling on the mechanical properties and microstructure of electron beam melted Ti-6Al-4V specimens*, Additive Manufacturing, 22, pp 834-843
- [10] Liu S Shin Y C 2019 *Additive manufacturing of Ti6Al4V alloy: A review*, Materials & Design, 164, 107552